Carbohydrate Polymers 84 (2011) 1329–1336

Contents lists available at ScienceDirect

Carbohydrate Polymers

journal homepage: www.elsevier.com/locate/carbpol

Chitosan fibrous 3D networks prepared by freeze drying

Min Young Kim, Jonghwi Lee*

Department of Chemical Engineering and Materials Science, Chung-Ang University, 221 Heukseok-dong, Dongjak-gu, Seoul 156-756, South Korea

ARTICLE INFO

Article history:
Received 20 July 2010
Received in revised form 18 January 2011
Accepted 19 January 2011
Available online 25 January 2011

Keywords:
Electrohydrodynamic jetting
Electrospraying
Electrospinning
Chitosan
Nonwoven fabrics
Fibers

ABSTRACT

Nonwoven fabrics and structured particles prepared by electrohydrodynamic jetting have been attracting increasing attention in various research areas. Chitosan has been known as a poorly spinnable polymer, often electrospun using a mixed solution of polyethylene glycol. Herein, we report that a combination of electrospraying and subsequent freeze drying can produce chitosan fibrous 3D network structures from low concentration chitosan solutions, well below fiber forming concentrations. Nanoparticle suspensions of chitosan were first fabricated by a controlled electrospraying process and then freeze drying assembled the nanoparticles into fibrous networks. The formation of a columnar ice phase and subsequent drying produced chitosan fibrous structures of a few microns in diameter. The X-ray diffraction results and the surface morphologies of the fibers indicate a unique fiber formation mechanism of biaxial compression. This technique can prepare nonwoven fabrics from nanoparticles, which lead to novel opportunities in applications including tissue engineering, cell or drug delivery, and membranes.

1. Introduction

Electrohydrodynamic jetting is used to prepare fibers (electrospinning) and particles (electrospraying) (Agarwal, Wendorff, & Greiner, 2009; Dosunmu, Chase, Kataphinan, & Reneker, 2006; Greiner & Wendorff, 2007; Ho, Park, Park, & Lee, 2009; Jaworek & Sobczyk, 2008; Lopez-Herrera, Barrero, Lopez, Loscertales, & Marquez, 2003; Teo & Ramakrishna, 2006). This process uses electrostatic forces applied to the surface of the jetting solution to fabricate various nanostructures by overcoming the surface energy of polymer solutions (Barrero, Ganan-Calvo, Davila, Palacio, & Gomez-Gonzalez, 1998; Ganan-Calvo, 1999; Lopez-Herrera et al., 2003). As the concentration of the polymer solution increases, particle structures become beads and fiber structures (Shenoy, Bates, Frisch, & Wnek, 2005). At a relatively high polymer concentration, electrohydrodynamic jetting results in electrospinning, which has been applied to the preparation of various nonwoven polymer fabrics. The electrospun fibers have potential applications in numerous research and development fields.

Electrospinning methods offer convenient control of spinning steps. Aligned or randomly oriented fibers, core–shell structured fibers, and conjugated or alternating fibers can all be produced through electrospinning (Agarwal et al., 2009; Greiner & Wendorff, 2007; Loscertales et al., 2002; Park & Lee, 2010). Polymers demonstrating a wide range of physical and chemical properties have been successfully spun. However, this convenient method is often limited by the intrinsic properties of polymers and their solutions. For example, several polymers are often electrospun using a mixed solution of polyethylene glycol, which is easily spinnable (Li & Hsieh, 2006; Ohkawa, Cha, Kim, Nishida, & Yamamoto, 2004). Furthermore, when the diameters of the fibers cannot be reduced enough, the resulting fiber morphology is not much different from in the morphology obtained from conventional solution spinning techniques (Hirano, 2001).

The second most abundant polysaccharide, chitosan, has beneficial properties such as its biodegradability, biocompatibility, mucoadhesiveness, and adsorption and antimicrobial properties, which make this material attractive in various applications (Crini & Badot, 2008; Rinaudo, 2006; Sezer et al., 2008). However, a serious drawback of chitosan is its poor processability (spinnability) originating from its molecular structure. Chitosan has strong intermolecular hydrogen bonding, rigid D-glucosamine structures, and high crystallinity. A common solution to address these drawbacks is random deacetylation, which results in reduced molecular weight and crystallinity.

The electrohydrodynamic jetting technique has been used with chitosan to prepare particles, fibers, and membranes (Agboh & Qin, 1997; Guo, Xia, Wang, Song, & Zhang, 2005; Hirano, 2001; Marsano et al., 2005; Tang, Zhang, Wang, Fu, & Zhang, 2009). However, chitosan is relatively difficult to electrospin due to a lack of chain entanglement (Li & Hsieh, 2006; Ohkawa et al., 2004; Zhang et al., 2009). The concentrations of chitosan solution for spinning cannot be increased easily due to low solubility and high viscosity. At concentrations above 3%, chitosan becomes gelled and at concentrations below 2%, particles are usually produced. Thus, it has been reported that fibers are difficult to prepare from electrospin-

* Corresponding author. Tel.: +82 2 816 5269; fax: +82 2 824 3495.
E-mail address: jong@cau.ac.kr (J. Lee).

0144-8617/$ – see front matter © 2011 Elsevier Ltd. All rights reserved.
doi:10.1016/j.carbpol.2011.01.029

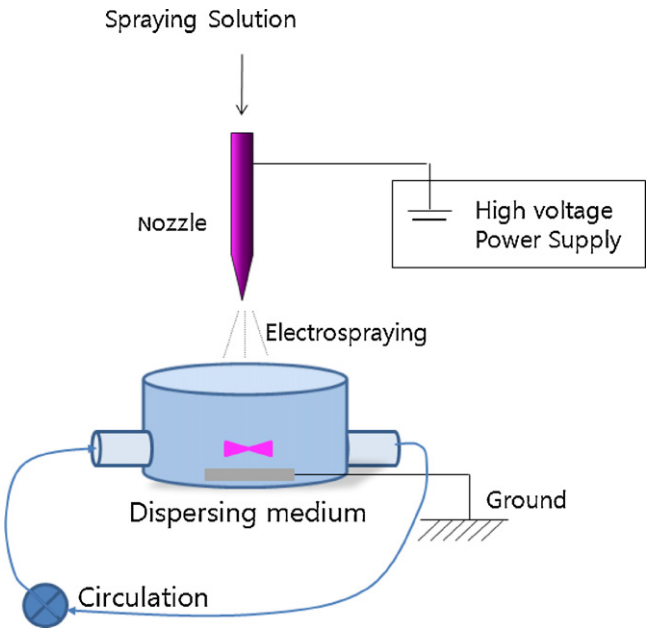

Fig. 1. Schematic of the electrohydrodynamic spraying apparatus.

ning of chitosan even in aqueous acetic acid (Li & Hsieh, 2006). Instead of pure chitosan, a mixture of chitosan and another polymer (often polyethylene glycol) is often used to prepare nonwoven fabrics (Agboh & Qin, 1997; Choi, Kim, Pak, Yoo, & Chung, 2007; Funakoshi et al., 2005; Li & Hsieh, 2006; Ohkawa et al., 2004; Ojha et al., 2008).

In this study, without using an extra polymer, pure chitosan fibrous structures (nonwoven fabrics) were prepared from a low concentration chitosan solution. We used a freeze drying process consisting of electrospraying (particle formation) and subsequent freeze drying (fiber formation (stretching)). As a result, freeze drying can assemble chitosan nanoparticles into fibrous 3D network structures. In similar recent researches on ceramic materials, freeze drying has prepared extraordinarily tough lamellar composite structures from metal oxide particles and polymers, which proved that freeze drying can be used as a fabrication method (Deville, Saiz, Nalla, & Tomsia, 2006; Deville, Saiz, & Tomsia, 2007; Gutierrez, Ferrer, & del Monte, 2008; Ogasawara, Shenton, Davis, & Mann, 2000; Zhang, Long, & Cooper, 2005).

2. Materials and methods

2.1. Materials

Chitosan (medium molecular weight, deacetylation 75–85%, viscosity 200–800 cP (1% in 1% acetic acid)) and tripolyphosphate (TPP) were purchased from Sigma–Aldrich (St. Louis, MO, USA). Acetic acid (99.5%) was received from Samchun Pure Chemical (Pyongtack, Gyeonggi, South Korea). HPLC grade water was obtained from J.T. Baker (NJ, USA). Phosphate buffer solution (PBS, pH 7.4) was prepared using Na_2HPO_4 and NaH_2PO_4 (Sigma–Aldrich). All of the materials were used as received without further purification.

2.2. Electrohydrodynamic spraying and freeze drying

The experimental apparatus is shown in Fig. 1. The jetting solution was stored in a 5 ml syringe (Becton, Dickinson and Company, NJ, USA) and sprayed into a T-type glass chamber (dispersing medium bath) through a 26 gauge stainless steel nozzle (I.D. 0.21 mm, O.D. 0.46 mm). The flow rate was controlled by a syringe pump (KDS 100 model, KdScientific, Holliston, MA, USA). A positive DC voltage supply (0–35 kV/5 mA, ConverTech, NT_{SEE}, Gwangju, South Korea) was connected to the nozzle. In the T-type glass chamber, the coagulation liquid was circulated by a fixed quantity metering pump (MP-100, EYELA, Tokyo, Japan) at a rate of 365 ml/h.

The electrospraying solution was a 1 wt% chitosan solution unless otherwise stated and was prepared by dissolving chitosan in 0.9 wt% acetic acid. The coagulation liquid (dispersing medium) contained 30 ml of water, TPP solutions, or PBS buffer solutions. The applied voltage was 8 kV and the flow rate was 1 ml/h unless otherwise stated. After 2 ml of the chitosan solution (1 wt%) was electrosprayed, the suspension was centrifuged for 30 min to concentrate the suspension using a MICRO 17R+ (Hanil Science Industrial, Incheon, South Korea, 10,000 rpm). The concentrated suspensions were frozen in liquid nitrogen (or in a freezer), and then freeze dried for 2 days using a freeze dryer FD-1000 (EYELA, Tokyo, Japan) (fiber formation step). To investigate the effects of crosslinking by TPP, 2 ml of the chitosan solution was electrosprayed into a 0.02 wt% TPP solution (dispersing medium) and then the suspension was freeze dried after stirring for 5 min.

For comparison, fiber structures developed from a simple precipitation method without electrospraying were prepared. Two milliliters of the chitosan solution (1 wt%) was added to 30 ml of water and the resulting solution was then homogenized at 17,000 rpm using a T8 ULTRA-TURAX (Homogenizer, IKA®-WERKE, Staufen, Germany) for 1 h. Then, the suspension was treated by the same freeze drying procedure described above.

2.3. Characterizations

The sizes of the chitosan particles were analyzed using a LA-910 (Horiba, Kyoto, Japan) laser light scattering analyzer (Mie & Fraunhofer, relative refraction index = 1). The sonication power of the particle size analyzer was 40 W (39 kHz) and the circulation rate was 340 ml/min. Volume-averaged particle sizes of the nanosuspension were obtained.

The crystallinity of the chitosan fibers was measured using wide angle X-ray diffraction with a D/max-2500/PC (Rigaku Co., Japan, 2°/min). The morphology of the chitosan particles and fibers was investigated using a scanning electron microscope (SEM, S-4700, Hitachi, Ltd., Tokyo, Japan) and an atomic force microscope (XE-100 AFM, PSIA Co., South Korea). Particle samples for SEM and AFM were prepared by placing a drop of the suspension containing chitosan particles on a glass slide and subsequent vacuum drying. The samples were coated with Pt–Pd at a speed of 6.7 nm/min for 120 s and evaluated at 4 kV. The AFM samples were scanned in the tapping mode. Etched silicon tips on a cantilever (NSC15, Park Systems, Korea) with a force constant of 40 N m^{-1} (specified by the manufacturer) were used.

3. Results

3.1. Preparation of chitosan nanoparticles

We first tried to prepare chitosan nanoparticles using electrohydrodynamic jetting. Electrohydrodynamic spraying (electrospraying) has been utilized for drug delivery researches for more than a decade, but it is still not well established compared to electrospinning (Jaworek & Sobczyk, 2008; Xie, Lim, Phua, Hua, & Wang, 2006; Xu & Hanna, 2006). Well dispersed polymeric nanoparticle aqueous suspensions are difficult to prepare by electrospraying into a water bath. Once particles lose their surface electrostatic charge upon grounding (water), they tend to easily aggregate. Aggregation becomes more pronounced as the production of nanoparticles

Table 1
Volume-averaged particle sizes of chitosan particles prepared by electrospraying.

Voltage (kV)	Dispersing medium[a]	Mean particle size (μm)
4	Distilled water	0.73 (±0.22)
8	Distilled water	0.34 (±0.53)
12	Distilled water	0.58 (±0.14)
12	0.02 wt% TPP solution	19.1 (±11.4)
12	0.2 wt% TPP solution	43.66 (±44.43)
12	0.001 M buffer solution	0.27 (±0.42)
12	0.1 M buffer solution	4.48 (±7.69)
14	Distilled water	0.97 (±0.20)

[a] Ground, where sprayed particles were collected.

continues. This was an important problem for us to overcome in order to prepare a significant amount of well dispersed nanoparticles in water. Therefore, the preparation apparatus was carefully adjusted and proper conditions for the fabrication of the chitosan nanoparticles were determined. Fig. 1 shows the apparatus developed for the electrospraying of chitosan. Chitosan droplets formed by electrohydrodynamic forces travel into a dispersion medium (water), where they can exist as well dispersed particles.

Table 1 shows the volume-averaged sizes of the chitosan particles obtained in various dispersing media when the applied voltage was 12 kV. Since the composition of the dispersing medium does not significantly change the electrohydrodynamic jetting conditions, the primary droplets formed from the nozzle were probably similarly sized (Barrero et al., 1998; Ganan-Calvo, 1999). The property of the dispersing medium (the ground) is not a determining factor according to the theoretical principles of droplet formation (Barrero et al., 1998; Ganan-Calvo, 1999). Thus, the differences in the sizes of the 12 kV cases in Table 1 are mainly a result of the aggregation behavior of each sample.

In distilled water, chitosan solution droplets become physical hydrogel particles due to the poor solubility of chitosan in water. They are relatively well dispersed and may be in a swollen state. A small amount of TPP induced crosslinking and aggregation of chitosan particles, resulting in a mean particle size well above 1 μm. The particle size distribution of the sample was relatively wide, which implies that the change was caused by inter-particle crosslinking due to TPP. A small amount of buffer salts (0.001 M) helped to disperse the chitosan particles, but a further increase in the buffer concentration induced the aggregation of particles, resulting in a mean particle size above 1 μm. This might be due to the shielding effect of buffer against the surface charges of amine groups in chitosan particles. These studies show us that the chitosan particles can readily assemble together depending on environmental conditions, which may be the reason why it is possible to fabricate fibrous structures from them.

The effect of the applied voltage on the mean particle size above the critical voltage necessary for the formation of a Taylor cone is shown in Table 1. According to theoretical and experimental studies, the size of the primary particles formed at the tip of the jetting nozzle can be reduced by increasing the applied voltage (Ganan-Calvo, 1999; Jaworek & Sobczyk, 2008). Indeed, a reduction in the particle size is found in the 4 and 8 kV cases. However, a further increase in the applied voltage to 12 and 14 kV resulted in increased particle sizes. It is likely that the second fission of droplets occurs and the smaller primary droplets formed at a higher applied voltage lead to increased aggregation in dispersing medium, resulting in an increase of the average size of solidified particles.

Fig. 2 shows the particle size distribution curves of the different voltage cases. As expected, the 8 kV case shows a strong peak in the smallest size range (near 200 nm). However, it also has a small but significant population above 1 μm. In the other cases of 4, 12, and 14 kV, the population above 1 μm is more significant, which seems to be related to aggregation. The particle size distribution of the 12 kV case is relatively wide, possibly indicating significant aggregation. Different dispersion media also provide different particle size distributions as can be seen in Fig. 2b and c, which reflect the results of Table 1. Although the samples have similar droplet formation process at the tip of an electrospraying nozzle, the dif-

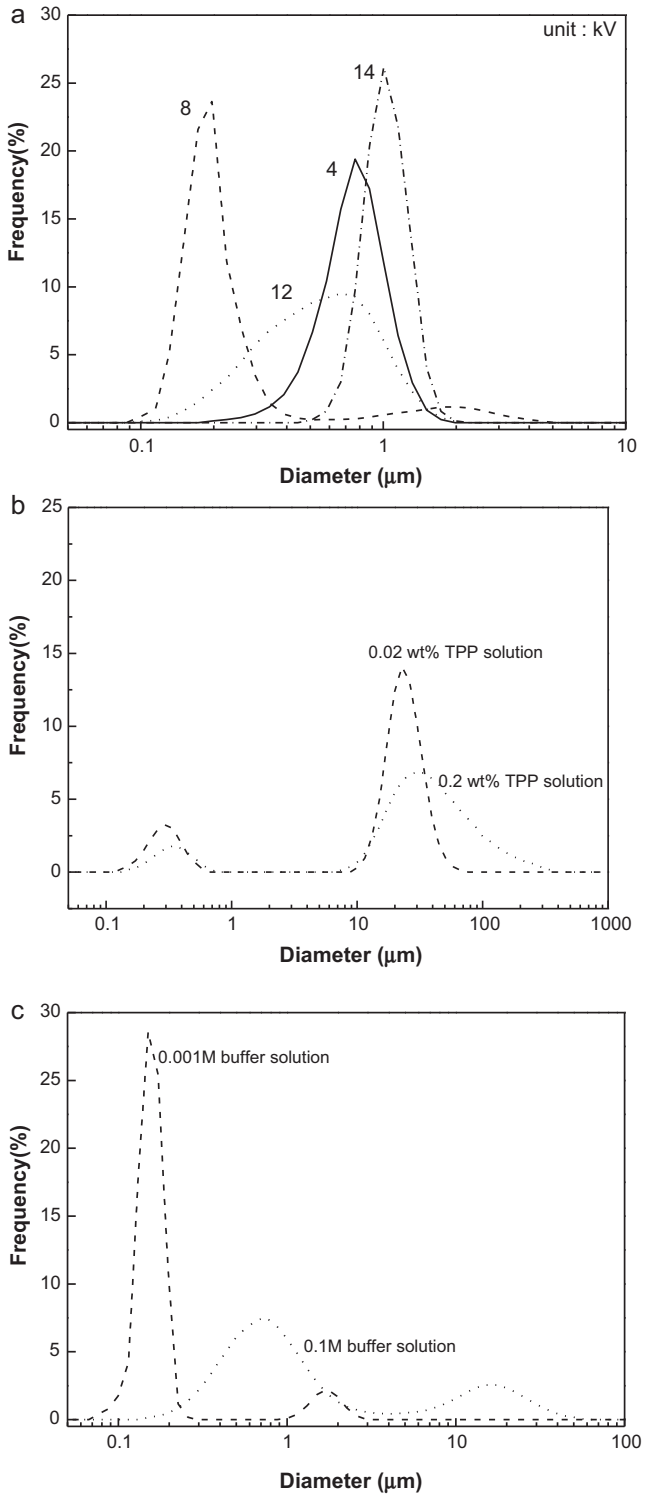

Fig. 2. Effects of (a) applied voltage, (b) TPP concentration, and (c) phosphate buffer concentration on the particle size distribution of the chitosan particles. The numbers in (a) represent the applied voltages (kV).

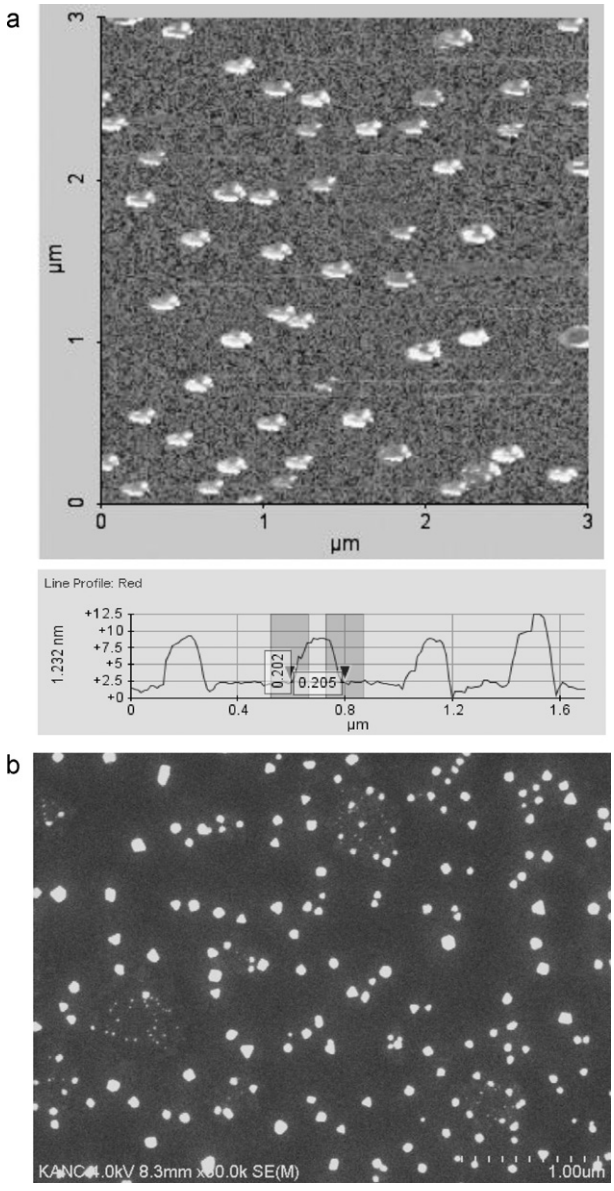

Fig. 3. (a) AFM image with a line profile and (b) SEM images of chitosan particles prepared at 8 kV.

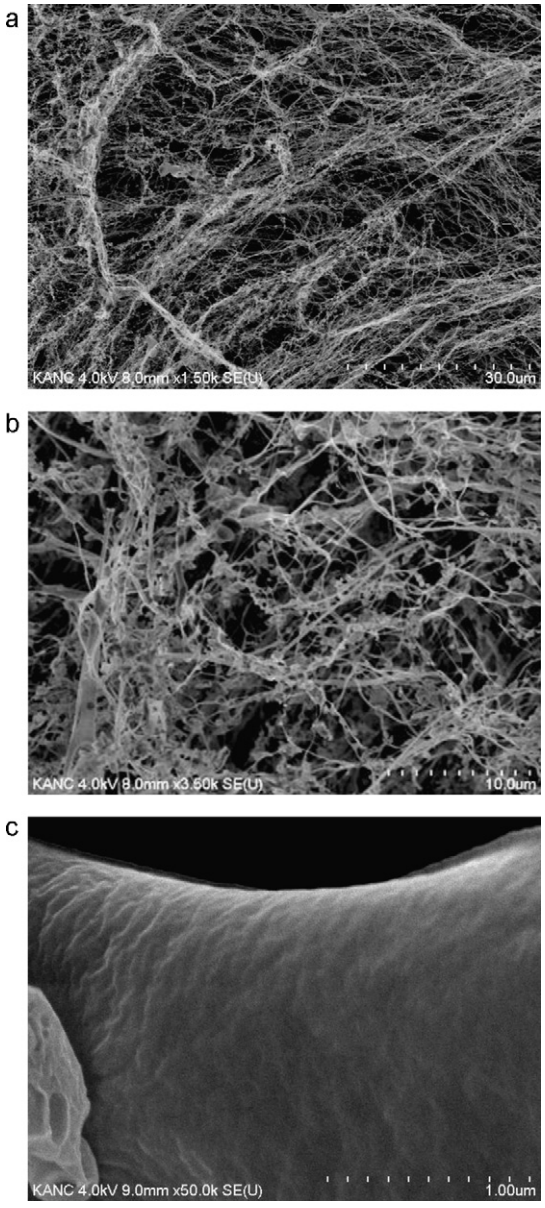

Fig. 4. SEM micrographs of (a) and (b) surface region of chitosan nonwoven fabrics after freeze drying, and (c) the surfaces of the fibers [preparation conditions: 8 kV, 1 ml/h, distilled water, freeze drying of 1.32 wt% chitosan suspension (fast freezing using liquid nitrogen), 0.34 μm].

ferences in aggregation seem to result in the differences in particle size distribution.

The differences in particle size and distribution are supported by SEM observation (Fig. 3). Fig. 3 shows the particles of chitosan prepared by electrohydrodynamic jetting after vacuum drying (not freeze drying). AFM and SEM micrographs show the existence of 100–300 nm sized particles, which corresponds to the submicron peak of the 8 kV case observed in Fig. 2.

The particles appear to be slightly imperfectly spherical. This morphology may originate from shrinking of swollen chitosan particles during drying. Indeed, the height of vacuum dried particles in Fig. 3a is only about 12 nm, indicating significant swelling in a water dispersion state. However, the aggregation of primary particles could be another reason. Although the particles size distributions in Fig. 2 suggest 100–300 nm primary particle size, the actual size of primary particles could be even smaller, and the 100–300 nm particles could be aggregates, which the relatively large standard deviations in particle size results (Table 1) may suggest.

3.2. Chitosan fibrous structures

The original objective of our research was the development of a versatile preparation method of well-dispersed drug delivery carriers for an oral solid dosage form, which is the most popular and economical form of delivery. Therefore, after the relatively well-dispersed nanoparticles were obtained at 8 kV, freeze drying was chosen for solidification. Freeze drying is known to be a convenient unit operation to dry drug nanosuspensions into redispersable powders. After freeze drying, interestingly, we observed fine fibrous structures developed during the freeze drying of chitosan suspensions.

Fig. 4 shows the typical fibrous structures obtained by electrospraying and subsequent freeze drying. The average diameter of a strand was 0.5–3 μm. Fibrils are often interconnected with each other. The nonwoven fabric structure does not have bead-string structures, which are often found in electrospun fibers (Li & Hsieh,

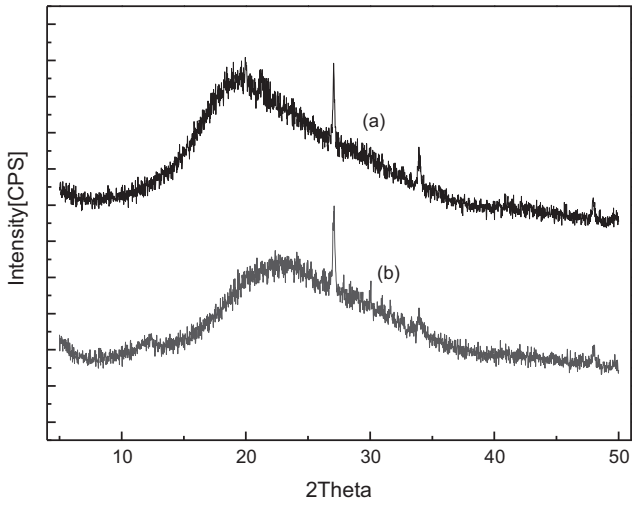

Fig. 5. X-ray diffraction results for (a) freeze dried chitosan fibers after electrospraying and (b) vacuum dried chitosan particles after electrospraying.

2006; Ohkawa et al., 2004). On the other hand, the diameters seen in Fig. 4 vary along the fiber direction, which is not common in electrospun or conventional solution-spun fibers. The surface area of the fibers was measured to be $17.8 \pm 0.39\ m^2/g$ by a BET surface area analyzer (ASAP-2010, BET Micromeritics, Morcross, USA).

The surfaces of the fibers are different from those of conventional fibers (Funakoshi et al., 2005; Hirano, 2001; Li & Hsieh, 2006; Ohkawa et al., 2004). Fig. 4c shows that the surfaces of the fibers do not have any significant features (textures) resulting from a stretching process along the fiber direction, like those found in most chitosan fibers (Choi et al., 2007; Funakoshi et al., 2005; Li & Hsieh, 2006; Ohkawa et al., 2004). Fibers undergo large deformations during spinning along the fiber direction and therefore, longitudinal features are often left on the surfaces of the fibers (Hirano, 2001; Rubner & Rutledge, 2007). The crystallinity of polymers is normally improved by fiber stretching.

The absence of significant fiber stretching could be further supported by the XRD results shown in Fig. 5. Conventional fiber spinning induces crystallization, resulting in alterations of X-ray diffraction patterns. In the cases of chitosan fibers produced from wet spinning, peaks near 10° and 20° (2θ) develop with fiber stretching (Agboh & Qin, 1997; Choi et al., 2007). The XRD pattern of the fibers (freeze dried) in Fig. 5a is not significantly different from that of the particles (vacuum dried) in Fig. 5b. Instead of strong crystalline peaks in the conventional chitosan fibers (Agboh & Qin, 1997; Choi et al., 2007), a broad amorphous peak near 20° was observed. Therefore, it seems that both chitosan fibers and particles have a similar amorphous molecular structure, which will result in unique physical properties such as significant plastic deformation different from those of conventional non-woven fabrics.

The position of the amorphous halo shifted to a slightly smaller degree (longer spacing) after freeze drying. It is unclear whether this difference is meaningful in interpreting the amorphous structure of the chitosan materials, but it may be related to the relatively porous structures caused by the fast removal of water in the cryoconcentrate or chitosan phases without proper volume shrinkage during freeze drying. The small sharp peaks at 27° and 34° appear to be related with the small molecules remained in chitosan (possibly small molecules from the deacetylation of chitosan).

3.3. Preparation conditions

The formation of chitosan fibers by electrospraying and subsequent freeze drying was dependent on suspension concentration, freezing rate, etc. Fig. 6a shows the effect of the suspension concentration. Too high concentrations led to relatively poorly developed fibrous structures and more pronounced film type structures. A proper volume ratio of water to chitosan particles led to a proper development of the phase boundary, which can generate the fiber spinning force. This is similar to the previous researches on the directional freezing of ceramic materials (Deville et al., 2006, 2007b; Gutierrez et al., 2008; Ogasawara et al., 2000; Zhang et al., 2005).

Fig. 6b shows that relatively slow freezing of the chitosan suspension in a freezer (−24 °C) resulted in a poorly developed fiber structures. Fast freezing and the resulting small columnar ice phases, which could be directionally developed, are necessary for the development of fiber structures.

Chitosan nanoparticles can be prepared by a precipitation method (Agnihotri, Mallikarjuna, & Aminabhavi, 2004). A suspension with the same chitosan concentration as the electrosprayed suspension was prepared and freeze dried to investigate whether the electrospraying step is necessary for fiber formation. The volume-averaged size of the chitosan particles prepared by the precipitation method was 0.95 (±0.43) μm. The resulting fibrous structures after freeze drying (same method as Fig. 4) in Fig. 6c were similar to those shown in Fig. 6b. Therefore, if the size and concentration of chitosan particles can be carefully controlled, the development of a fibrous structure may be possible even without electrospraying. However, in our repeated attempts, successful fiber formation similar to Fig. 4 could not be achieved, possibly due to the limited controllability of the precipitation method. The use of a stabilizer in the precipitation method, which can control the size of chitosan particles as well as change the phase separation behavior of suspension during the freezing and drying steps, was not utilized in here.

An interesting morphology was observed when TPP crosslinked chitosan particles were freeze dried (Fig. 6d). This chemical crosslinking can induce aggregation of primary particles but prevent further morphological transformation such as transforming particles to fibrous structures. In Fig. 6d, connected structures are seen but fibrous structures are not. The aggregation of particles produced structural connectivity but chemical crosslinking prevented significant fiber formation during the freeze drying. As a result, the chitosan structure in Fig. 6d is significantly different from the other structures shown in Figs. 4 and 6.

We also investigated the influence of the steps preceeding the freeze drying step. The conditions used in the centrifuge step and the storage time were examined in detail. No significant differences were observed in the particle morphologies and no evidence of fiber formation before freeze drying was found. These examinations lead us to conclude that fiber formation (stretching) occurs primarily during the freeze drying step.

4. Discussion

Freeze drying has been the first choice drying method for nanoparticles, particularly for good redispersability. Only recently, it has been reported that freeze drying technique could fabricate lamellar structures of nanoparticles under a controlled condition (Deville et al., 2006, 2007b; Gutierrez et al., 2008; Ogasawara et al., 2000; Zhang et al., 2005). Our study shows the possibility of fibrous network formation by freeze drying chitosan nanosuspensions for the first time. The nonwoven fabrics of chitosan could be prepared without overcoming its spinnability issues.

The common misconception that freeze drying retains the intact structures of solutions, suspensions, or swollen states is not true in many cases. Freezing causes phase separation as water freezes into ice crystals while excluding solutes and particles into a cryo-

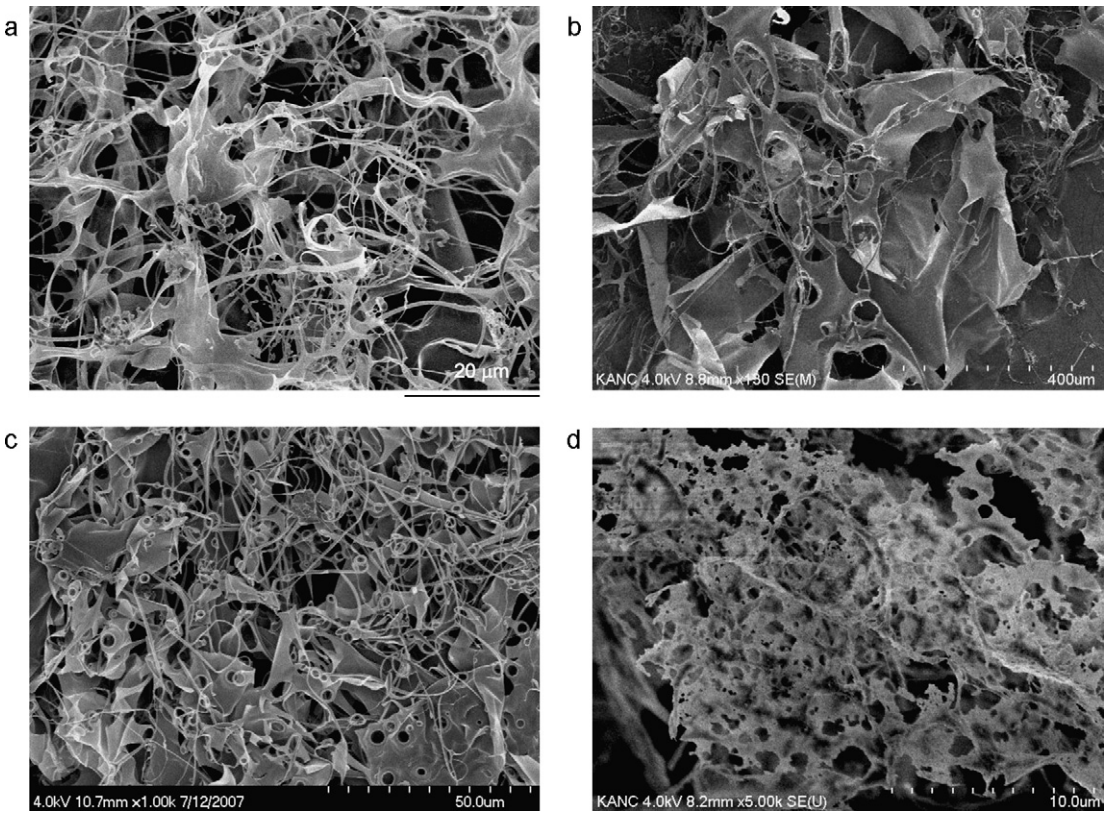

Fig. 6. Chitosan fibers prepared by various different methods: (a) 2.60 wt% chitosan suspension, frozen in liquid nitrogen (*higher concentration*), (b) 1.32 wt% chitosan suspension, frozen in a freezer (−24 °C) (*slow freezing rate*), (c) chitosan particles from precipitation, and (d) 1.32 wt% chitosan suspension, 0.02 wt% TPP solution, frozen in liquid nitrogen (*crosslinked particles*).

concentrated liquid phase (Abdelwahed, Degobert, Stainmesse, & Fessi, 2006; Lee & Cheng, 2006). Significant mechanical stress develops around the cryo-concentrated liquid phase. In particular, interfacial regions between more than 2 ice phases will experience a stress state close to biaxial compression. The perfect biaxial compression is identical to uniaxial tension (Fig. 7). As a result, fiber formation could occur during freeze drying. Triple junctions among three ice phases may be more effective in producing fibrous structures than interfaces between two phases. To promote fibrous structures instead of connected sheet structures, development of many small columnar ice crystallites may be necessary, which results in more triple or quadruple junctions among the ice crystallites.

Dissolved polymer nanoparticles tend to be excluded from the ice phase during freezing, since the solubility of a solute in ice is almost negligible. The flat interface of the freezing front excludes solutes and develops a significant concentration gradient. The overall freezing rate is determined by the rate of heat extraction, and the local growth rate is limited by the low liquid diffusivity. Therefore, above a certain freezing rate, the flat freezing front adapts to a dendritic shape, which then becomes columnar or lamellar structures later. The formation of columnar structures is

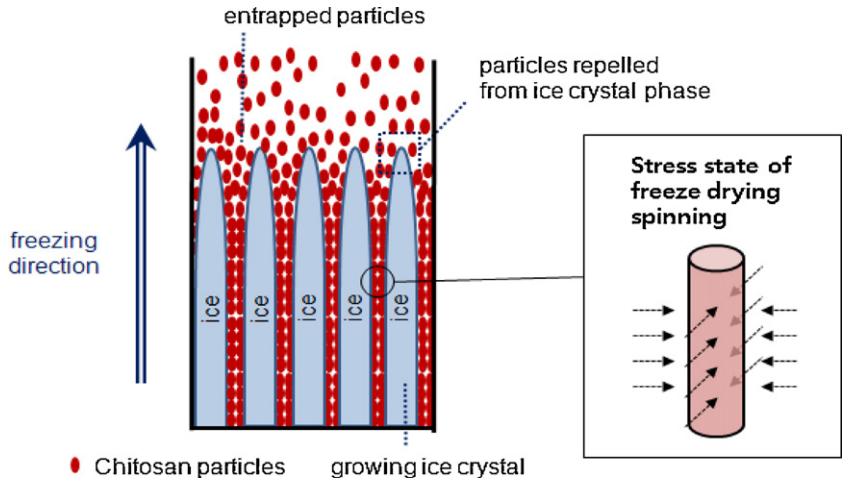

Fig. 7. Fiber formation mechanism of chitosan particles in the freeze drying process.

known as Mullins–Serkerka instability (Hadji, 2003). Kurz and Fischer suggested that dendrite morphology is defined by sinusoidal perturbations at the solid–liquid interface (Kurz & Fisher, 1981). Simple particle pinning can cause the same dendrites (Deville, Saiz, & Tomsia, 2007).

For the fibrous network formation, columnar ice phases are preferred to lamellar ice crystals. As previously reported, the growth of columnar ice crystal mainly occurs when the freezing rate is fast enough. In here, the fast freezing rate was achieved by dipping into liquid nitrogen, and reproducible fibrous network formation could be observed. Fast freezing also induce smaller ice crystals, resulting in finer fibrous structures as can be seen in Fig. 4.

The concentration of chitosan particles was a critical parameter in Figs. 4 and 6. The mobility and the interparticular distance of the chitosan particles can influence the growth of columnar ice crystals and the formation of fibrous networks. A proper concentration of cryo-concentrated phases seems to be necessary as well for the formation of continuous chitosan phases. Otherwise, biaxial compression could not induce 1D structure formation of chitosan molecules. Therefore, freeze drying and the related biaxial compression appear to induce linear aggregation of chitosan particles and fibrous structure formation, as seen in Fig. 7.

The proposed mechanism in Fig. 7 is similar to what has been observed in directional freezing (ice templating) experiments producing lamellar structures (Deville et al., 2006, 2007b; Gutierrez et al., 2008; Lee, Chung, & Lee, 2010; Ogasawara et al., 2000; Zhang et al., 2005). They employed relatively slow freezing rate and the final structures of the directional freezing experiments were porous films. However, the basic mechanism of the ice crystal phase in the directional freezing experiments is similar to our cases.

The 'spinnability' of the jetting solution, which is a function of various factors including viscosity and chain entanglement, does not play a major role in this novel method (Paul, 1968; Shenoy et al., 2005). Instead, the phase separation and morphology of the ice phases, and the structure of the interfacial region play major roles in determining the morphology of the fibers. Low crystallinity and more connections between fibrous strings are expected in this fiber formation mechanism, which could provide unique combination of physical properties different from the conventional nonwoven fabrics.

We implemented a simple freeze drying process without a secondary drying step. A post annealing step after freezing or control of primary and secondary drying conditions, which are often used in the freeze drying process, may improve the fiber formation process (Abdelwahed et al., 2006; Searles, Carpenter, & Randolph, 2001).

This study opens up a possibility of chitosan fibrous network formation by freeze drying. This method can fabricate 3D nonwoven fabrics of not only non-spinnable polymers but also core/shell, anisometric and other structured particles developed by electrospraying. Therefore, with this method, the conventional particle preparation processes can take one more step toward the preparation of intelligent releasing membranes, sensor devices, scaffolds, drug or cell delivery systems, etc.

5. Conclusions

Electrospinning of chitosan into nonwoven fabrics is challenging because of the high viscosity and low chain entanglement density of chitosan solutions, which historically have required an additional polymer for electrospinning. We developed a novel preparation method of fibrous 3D networks consisting of electrospraying and subsequent freeze drying that successfully generated pure chitosan fibers. Electrospraying produced well dispersed chitosan nanoparticles and freeze drying assembled them into fibrous structures. The fiber formation relies on various processing parameters such as the type of dispersing medium of the nanoparticles, the chitosan concentration, and the freezing rate. Based on the SEM and XRD results, the fibers did not show significant stretching-induced characteristics. This processing technique can be used for the formation of fibrous 3D networks from non-spinnable polysaccharide polymers.

Acknowledgements

This work was supported by a Korea Science and Engineering Foundation (KOSEF) grant funded by the Korean Government (MEST) (No. 2009-0079798) and the Ministry of Health and Welfare in South Korea (A090996). MYK would like to thank the Human Resources Training Project for Strategic Technology (MKE and KOTEF).

References

Abdelwahed, W., Degobert, G., Stainmesse, S., & Fessi, H. (2006). Freeze-drying of nanoparticles: Formulation, process and storage considerations. *Advanced Drug Delivery Reviews*, *58*(15), 1688–1713.

Agarwal, S., Wendorff, J. H., & Greiner, A. (2009). Progress in the field of electrospinning for tissue engineering applications. *Advanced Materials*, *21*, 3343–3351.

Agboh, O. C., & Qin, Y. (1997). Chitin and chitosan fibers. *Polymers for Advanced Technologies*, *8*(6), 355–365.

Agnihotri, S. A., Mallikarjuna, N. N., & Aminabhavi, T. M. (2004). Recent advances on chitosan-based micro- and nanoparticles in drug delivery. *Journal of Controlled Release*, *100*(1), 5–28.

Barrero, A., Ganan-Calvo, A. M., Davila, J., Palacio, A., & Gomez-Gonzalez, E. (1998). Low and high reynolds number flows inside taylor cones. *Physical Review E*, *58*(6), 7309–7314.

Choi, C. Y., Kim, S. B., Pak, P. K., Yoo, D. I., & Chung, Y. S. (2007). Effect of N-acylation on structure and properties of chitosan fibers. *Carbohydrate Polymers*, *68*(1), 122–127.

Crini, G., & Badot, P. M. (2008). Application of chitosan, a natural aminopolysaccharide, for dye removal from aqueous solutions by adsorption processes using batch studies: A review of recent literature. *Progress in Polymer Science*, *33*(4), 399–447.

Deville, S., Saiz, E., Nalla, R. K., & Tomsia, A. P. (2006). Freezing as a path to build complex composites. *Science*, *311*(5760), 515.

Deville, S., Saiz, E., & Tomsia, A. (2007). Ice-templated porous alumina structures. *Acta Materialia*, *55*(6), 1965–1974.

Deville, S., Saiz, E., & Tomsia, A. P. (2007). Ice-templated porous alumina structures. *Acta Materialia*, *55*(6), 1965–1974.

Dosunmu, O. O., Chase, G. G., Kataphinan, W., & Reneker, D. H. (2006). Electrospinning of polymer nanofibres from multiple jets on a porous tubular surface. *Nanotechnology*, *17*, 1123–1127.

Funakoshi, T., Majima, T., Iwasaki, N., Yamane, S., Masuko, T., Minami, A., et al. (2005). Novel chitosan-based hyaluronan hybrid polymer fibers as a scaffold in ligament tissue engineering. *Journal of Biomedical Materials Research Part A*, *74*(3), 338.

Ganan-Calvo, A. M. (1999). The surface charge in electrospraying: Its nature and its universal scaling laws. *Journal of Aerosol Science*, *30*(7), 863–872.

Greiner, A., & Wendorff, J. H. (2007). Electrospinning: A fascinating method for the preparation of ultrathin fibers. *Angewandte Chemie-International Edition*, *46*(30), 5670–5703.

Guo, T. Y., Xia, Y. Q., Wang, J., Song, M. D., & Zhang, B. H. (2005). Chitosan beads as molecularly imprinted polymer matrix for selective separation of proteins. *Biomaterials*, *26*(28), 5737–5745.

Gutierrez, M. C., Ferrer, M. L., & del Monte, F. (2008). Ice-templated materials: Sophisticated structures exhibiting enhanced functionalities obtained after unidirectional freezing and ice-segregation-induced self-assembly. *Chemistry of Materials*, *20*(3), 634–648.

Hadji, L. (2003). Morphological instability induced by the interaction of a particle with a solid–liquid interface. *The European Physical Journal B*, *37*(1), 85–89.

Hirano, S. (2001). Wet-spinning and applications of functional fibers based on chitin and chitosan. *Macromolecular Symposia*, *168*, 21–30.

Ho, H., Park, S. H., Park, C. H., & Lee, J. (2009). Electrohydrodynamic spray drying using coaxial nozzles for protein encapsulation. *Polymer (Korea)*, *33*(4), 353–357.

Jaworek, A., & Sobczyk, A. T. (2008). Electrospraying route to nanotechnology: An overview. *Journal of Electrostatics*, *66*(3–4), 197–219.

Kurz, W., & Fisher, D. (1981). Dendrite growth at the limit of stability: Tip radius and spacing. *Acta Metallurgica*, *29*(1), 11–20.

Lee, J., & Cheng, Y. (2006). Critical freezing rate in freeze drying nanocrystal dispersions. *Journal of Controlled Release*, *111*(1–2), 185–192.

Lee, M. K., Chung, N.-O., & Lee, J. (2010). Membranes with through-thickness porosity prepared by unidirectional freezing. *Polymer*, *51*, 6258–6267.

Li, L., & Hsieh, Y. L. (2006). Chitosan bicomponent nanofibers and nanoporous fibers. *Carbohydrate research*, *341*(3), 374–381.

Lopez-Herrera, J. M., Barrero, A., Lopez, A., Loscertales, I. G., & Marquez, M. (2003). Coaxial jets generated from electrified Taylor cones. Scaling laws. *Journal of Aerosol Science*, *34*(5), 535–552.

Loscertales, I. G., Barrero, A., Guerrero, I., Cortijo, R., Marquez, M., & Ganan-Calvo, A. M. (2002). Micro/nano encapsulation via electrified coaxial liquid jets. *Science*, *295*(5560), 1695.

Marsano, E., Bianchi, E., Vicini, S., Compagnino, L., Sionkowska, A., Skopi ska, J., et al. (2005). Stimuli responsive gels based on interpenetrating network of chitosan and poly (vinylpyrrolidone). *Polymer*, *46*(5), 1595–1600.

Ogasawara, W., Shenton, W., Davis, S. A., & Mann, S. (2000). Template mineralization of ordered macroporous chitin–silica composites using a cuttlebone-derived organic matrix. *Chemistry of Materials*, *12*(10), 2835–2837.

Ohkawa, K., Cha, D., Kim, H., Nishida, A., & Yamamoto, H. (2004). Electrospinning of chitosan. *Macromolecular Rapid Communications*, *25*(18), 1600–1605.

Ojha, S. S., Stevens, D. R., Hoffman, T. J., Stano, K., Klossner, R., Scott, M. C., et al. (2008). Fabrication and characterization of electrospun chitosan nanofibers formed via templating with polyethylene oxide. *Biomacromolecules*, *9*(9), 2523–2529.

Park, C., & Lee, J. (2010). Alternating encapsulation of water-soluble components in a one-dimensional structure. *Macromolecular Materials and Engineering*, *295*(1), 22–25.

Paul, D. R. (1968). A study of spinnability in the wet-spinning of acrylic fibers. *Journal of Applied Polymer Science*, *12*(10), 2273–2298.

Rinaudo, M. (2006). Chitin and chitosan: Properties and applications. *Progress in Polymer Science*, *31*(7), 603–632.

Rubner, M. F., & Rutledge, G. C. (2007). Decorated electrospun fibers exhibiting superhydrophobicity. *Advanced Materials*, *19*, 255–259.

Searles, J. A., Carpenter, J. F., & Randolph, T. W. (2001). The ice nucleation temperature determines the primary drying rate of lyophilization for samples frozen on a temperature-controlled shelf. *Journal of Pharmaceutical Sciences*, *90*(7), 860–871.

Sezer, A. D., Cevher, E., Hatıpo lu, F., urtan, O., Ba, Z., scedil, A. L., et al. (2008). Preparation of fucoidan–chitosan hydrogel and its application as burn healing accelerator on rabbits. *Biological & Pharmaceutical Bulletin*, *31*(12), 2326–2333.

Shenoy, S. L., Bates, W. D., Frisch, H. L., & Wnek, G. E. (2005). Role of chain entanglements on fiber formation during electrospinning of polymer solutions: Good solvent, non-specific polymer–polymer interaction limit. *Polymer*, *46*(10), 3372–3384.

Tang, C., Zhang, Q., Wang, K., Fu, Q., & Zhang, C. (2009). Water transport behavior of chitosan porous membranes containing multi-walled carbon nanotubes (MWNTs). *Journal of Membrane Science*, *337*(1–2), 240–247.

Teo, W. E., & Ramakrishna, S. (2006). A review on electrospinning design and nanofibre assemblies. *Nanotechnology*, *17*, R89–R106.

Xie, J., Lim, L. K., Phua, Y., Hua, J., & Wang, C. H. (2006). Electrohydrodynamic atomization for biodegradable polymeric particle production. *Journal of Colloid and Interface Science*, *302*(1), 103–112.

Xu, Y., & Hanna, M. A. (2006). Electrospray encapsulation of water-soluble protein with polylactide effects of formulations on morphology, encapsulation efficiency and release profile of particles. *International Journal of Pharmaceutics*, *320*(1–2), 30–36.

Zhang, H., Long, J., & Cooper, A. I. (2005). Aligned porous materials by directional freezing of solutions in liquid CO_2. *Journal of the American Chemical Society*, *127*(39), 13482–13483.

Zhang, J. F., Yang, D. Z., Xu, F., Zhang, Z. P., Yin, R. X., & Nie, J. (2009). Electrospun core shell structure nanofibers from homogeneous solution of poly(ethylene oxide)/chitosan. *Macromolecules*, *42*(14), 5278–5284.